# Vapor-Liquid Equilibrium calculations at specified composition, density and temperature with the Perturbed Chain Statistical Associating Fluid Theory (PC-SAFT) Equation of State

*Alvaro Vidal*, Phoevos Koukouvinis, Manolis Gavaises*

School of Mathematics, Computer Science & Engineering, Department of Mechanical Engineering & Aeronautics, City University London, Northampton Square EC1V 0HB, United Kingdom

*Corresponding author: alvaro.vidal-roncero@city.ac.uk

**Keywords:** PC-SAFT, VT-FLASH, VT-STABILITY, Helmholtz energy minimisation

**Abstract.** In this study, the PC-SAFT equation of state is used for vapour-liquid equilibrium calculations using as independent variables the mixture composition, density and temperature. The method is based on unconstrained minimisation of the Helmholtz Free energy via a combination of the successive substitution iteration and Newton-Raphson minimisation methods with line-search; the positive definiteness of the Hessian is guaranteed by a modified Cholesky decomposition. The algorithm consists of two stages; initially, the mixture is assumed to be a single-phase and its stability is assessed; in case of being found unstable, a second stage of phase splitting (flash) takes place, in which the pressure of the fluid and compositions of both the liquid and vapor phases are calculated. The reliability of two different

methods presented in the existing literature, (i) using mole numbers and (ii) using the logarithm of the equilibrium constants as iterative variables, is evaluated in terms of both iterations and computational time needed to reach convergence, for seven test cases. These include both single and multicomponent Diesel fuel surrogates, known to give incomplete density information when using pressure and temperature as independent variables. Results show that iterating with the logarithm of the equilibrium constants also reproduces this issue, while it requires a smaller number of iterations than using with mole numbers as independent variables. However, the total computational time needed for the latter case is vastly inferior. Pressure and vapor volume fraction fields are discussed for a range of temperatures and densities, apart from the number of iterations needed during the flash calculation stage. A performance comparison is obtained against the Peng-Robinson equation of state, showing similar number of iterations required but a computational time increasing with the number of components. While for a single component PC-SAFT needs around 3 times more CPU time, for 4 components it is 6 times and for a mixture of 8 components it increases up to 14 times. Finally, the method is demonstrated to converge unconditionally for all conditions tested.

# 1 Introduction

The PC-SAFT equation of state (EoS)[1] is a theoretically derived model, based on perturbation theory[2-5], that requires five molecular-based parameters per component for associating fluids and only three for non-associating ones. Several advantages accrue when using the PC-SAFT EoS compared to a cubic EoS to calculate fluid properties. The PC-SAFT EoS more accurately predicts derivative properties, reducing errors by a factor of up to eight[6, 7], as compared to predictions with a cubic EoS, such as the Peng-Robinson[8] (PR) or Soave-Redlich-Kwong[9] (SRK) EoS. Density predictions with the PC-SAFT EoS exhibit six times lower error for a widely used surrogate such as dodecane[10] and half the error of those made with improved cubic equations, such as volume-translated versions[11]. The PC-SAFT EoS provides satisfactory agreement between calculated and experimental properties of reservoir fluids[12], natural gas[13] and asphaltene phase behaviour[14, 15].

There is a wide body of research comparing the accuracy of PC-SAFT against other EoS in multiphase problem, not exclusively on vapor-liquid equilibrium. Arya et al.[16] and more recently Vieira de Melo et al.[17] compared the PC-SAFT and Cubic-Plus-Association[18] EoS for phase calculations of asphaltenes present in crude oils where although both EoS gave acceptable results, the authors drew different conclusions. Gong et al.[19] compared Peng Robinson and PC-SAFT EoS while modelling the VLE of mixed refrigerants, with no clear advantage of using one EoS over another. The group of the authors (Vidal et al.[20]) used it to precisely model the volatility curves of Diesel surrogates up to eight components. Held et al.[21] modelled the solubility of sugar and sugar alcohols in ionic liquids, with reasonable accuracy. Peyvandi et al.[22] compared PC-SAFT, SAFT+CUBIC and PR EoS in the modelling of cryogenic fluids, with a clear disadvantage on the use of PR EoS. Economou et al.[23] investigated the VLE of gaseous mixtures related to carbon dioxide capture technologies using several EoS: SRK, PR, SAFT, and PC-SAFT EoS, among them PC-SAFT showed to be the most accurate when no binary interaction parameters (BIP) are used, although comparable accuracy was observed with a fitted BIP. However, most of the studies focus on the modelling of the phase equilibria as 'static' problems, without considering flowing systems, where the VLE problem is only part of the whole framework of Computational Fluid Dynamics simulations. Exceptions can be found on the latest work in Diesel sprays[24] or Diesel injections[25], however the fuel in these two cases is a single component or a pseudo-component and various techniques are used to work around the problem of density undefinition inside the saturation curve. Overall, there seems to be evidence to indicate that independent variables other than pressure and temperature are needed for complex computational fluid dynamics simulations.

The use of flash with density (or specific volume), temperature and composition is particularly useful whenever the pressure is unknown in an enclosed fluid and the phase change is a possibility. This happens in storage tanks design, during the capturing process of acid gases within oil reservoirs, or compositional reservoir simulations as there is no balance equation for pressure[26]. Also, in most real fluid equations of state, e.g. PC-SAFT or cubic EoS, the formulation is given depending naturally on density, or volume, temperature and composition, which also makes the choice of these variables for

70 the VLE calculations the most straight-forward. However, the existing body of research has only
71 employed pressure and temperature as independent variables for vapor-liquid equilibrium calculations
72 (PT-VLE) with the PC-SAFT EoS. Moreover, this method shows its limitations when the phase change is at
73 constant temperature and pressure, characteristic of single components. At constant pressure and
74 temperature, the state of the substance is undetermined at saturation conditions. However, the volume
75 (or density) changes provide the complete information. Lastly, this undefinition is not restricted only to
76 single components as it also appears in multicomponent mixtures for three phase systems[27] and those
77 composed of similar components, as will be shown in the results section for a Diesel surrogate.
78 A seminal study in this area is the one of Michelsen[28], who proposed the use of volume and
79 temperature as independent variables and the minimising the Helmholtz Free energy rather than the
80 Gibbs free energy for the multiphase problem. In addition, for pressure-explicit EoS this approach would
81 also avoid the need for an iterative process to find the density from pressure, as the pressure becomes
82 then an output of the minimisation process. This approach was then implemented for the stability
83 testing of hydrocarbon mixtures[29] using the SRK and the PR EoS with the tunnelling method[30]. Following
84 work used the successive substitution iteration (SSI) method and the PR EoS for the flash problem[31].
85 Over the past decade, studies related to minimising the Helmholtz free energy have been focused on
86 the Newton method[32]. Moreover, new frameworks have been published using variations of the
87 independent variables or decoupling the pressure equality condition during the flash stage[33]. Recently, a
88 framework using constrained minimisation has been also published Paterson et al.[34] in a generalized
89 form for specifications based on state functions other than pressure and temperature. There have been
90 works using density and temperature as independent variables for the calculation of the saturation
91 curves of single components in PC-SAFT[35, 36]. However, to author's best knowledge, stability analysis and
92 flash calculations using the this equation of state have been restricted to temperature *T* and pressure *P*
93 as independent variables[37].
94 Following the above limitation when pressure and temperature are used as independent variables,
95 the novelty of this work is the provision and assessment of the necessary numerical framework using

composition, density and temperature as input variables for the calculation of the vapor-liquid equilibrium within the structure of PC-SAFT, via the unconstrained minimisation of the Helmholtz Free energy.

In this study, the minimum of the molar Helmholtz Free energy *A* is calculated, defined in terms of density $\rho$, temperature $T$ and composition $\boldsymbol{z}$ as:

$$A(\boldsymbol{z},\rho,T) = \sum_{i=1}^{nc} z_i A_i^{id}(P(\boldsymbol{z},\rho,T),T) \; + \; A^{res}(\boldsymbol{z},\rho,T) \qquad (1)$$

Where the superscripts $id$ and $res$ refer to the ideal, given by the fundamental gas relation, and residual contributions of the Helmholtz Free Energy, modelled by PC-SAFT, respectively. This optimisation problem is solved via a combination of the successive substitution iteration (SSI) and the Newton minimisation method with a two-step line-search procedure, and the positive definiteness of the Hessian is guaranteed by a modified Cholesky decomposition[38]. The algorithm consists of two stages: first, the mixture is assumed to be in a single phase state and its stability is assessed via the minimisation of the Tangent Plane Distance (TPD); in case the minimum of the TPD is found to be negative, the mixture is considered unstable and a second stage of flash, i.e. phase splitting, takes place consisting on the search for the global minimum of the Helmholtz Free Energy. As a result, the pressure of the fluid and the compositions of both the liquid and vapor phases are calculated, from which every other thermodynamic property can be calculated, i.e. internal energy, enthalpy, entropy, speed of sound, etc, using the PC-SAFT[1]. The reliability of two different methods for the flash stage, NVL [39] and lnK[33], are evaluated in terms of both iterations and computing time needed to reach convergence. Following the work of von Solmons et al in VLE calculations[40], this work also assesses the computational time needed for its completion. The robustness of the algorithm is then tested with a mixture of 50 components and several other examples often found in the literature in two-phase equilibrium calculations. Particular attention is paid to the case of a single component and a Diesel surrogate, known to reproduce the already highlighted incomplete density information when using pressure and

120 temperature as independent variables. The overall accuracy of the VT-VLE algorithm combined with PC-
121 SAFT is tested against experimental data for a selected number of examples.
122
123 Following the above introduction, the second section provides the theoretical framework, describing
124 the Newton method, the stability and flash stages, the strategy followed for the initialisation, the initial
125 phase splitting in case the mixture is found unstable. The third section shows the results obtained for 7
126 test cases, providing the number of iterations and the computational time needed for convergence for
127 both the NVL and lnK methods. Then, the pressure and vapor volume fraction fields for selected
128 examples are discussed for a range of temperatures and densities, apart from the number of iterations
129 needed for convergence during the flash stage. A performance comparison is obtained against Peng-
130 Robinson, showing a substantial decrease in computational time when using the cubic than using the
131 molecular based EoS. Finally, validation cases against experiments are provided before concluding. The
132 Supplementary Information provides detailed information regarding the components used in this study
133 and the analytical derivatives needed for the algorithm.
134

# 2 Method

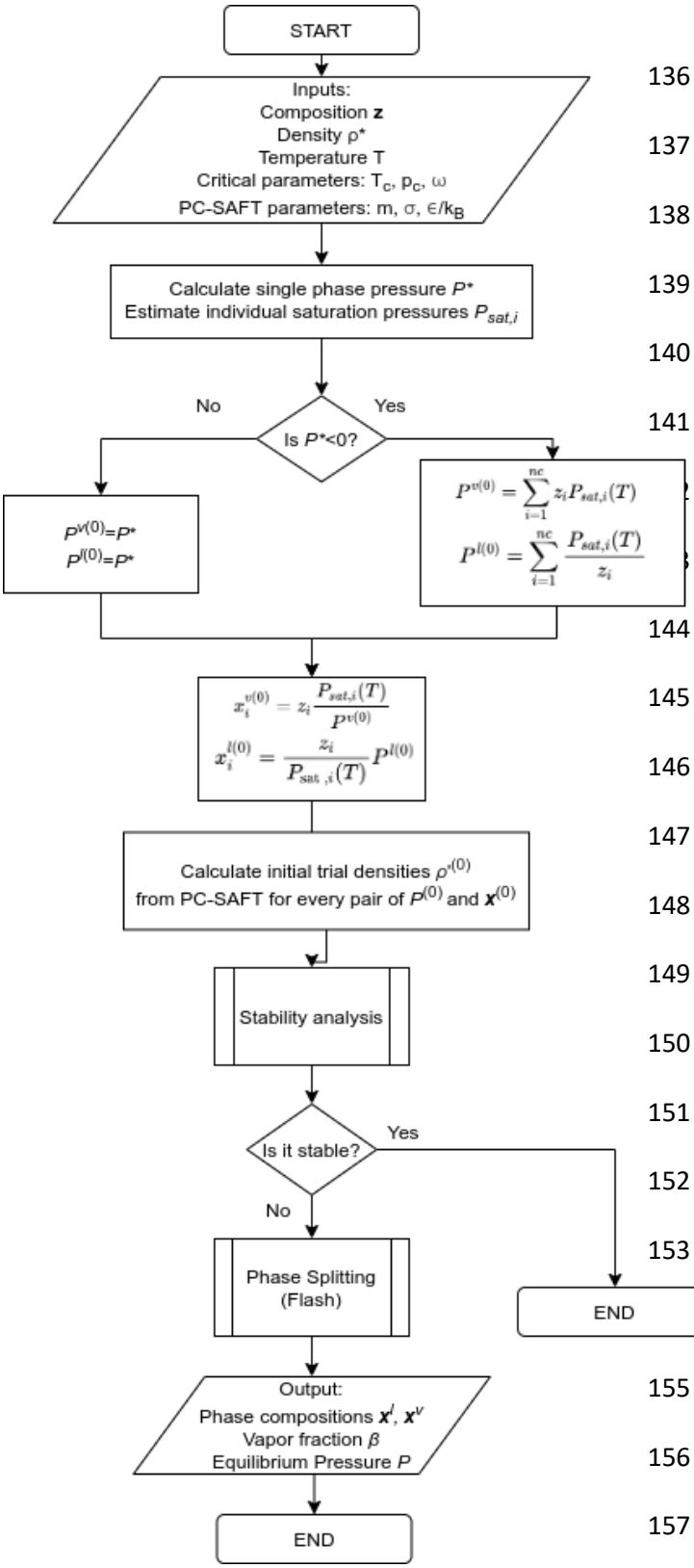


Scheme 1. General diagram for multiphase calculations

Any isolated system at constant density and temperature tends spontaneously to an equilibrium state while decreasing the Helmholtz free energy of the system, until the global minimum is reached, i.e. equilibrium. However, it may be the case that the state at which the equilibrium occurs is that of vapor and liquid coexisting. Thus, the amount of each phase, their composition and pressure need to be calculated.

In this work, the presented algorithm studies the stability of the homogeneous mixture using the PC-SAFT EoS for a given composition $z_1,..,z_{nc}$ with density $\rho$ and at a certain temperature $T$; in case it is found to be unstable, the vaporized fraction of the substance, the compositions of both phases and the resulting pressure in equilibrium are calculated via flash.

Both algorithms for the stability and flash stages have been already developed and published for the Peng Robinson EoS; only minor changes are needed for the PC-SAFT EoS regarding the convergence criteria in the iterations and constraints.

Scheme 1 shows the general diagram of the algorithm used in the multiphase calculations. For consistency, the whole algorithm is described here, and any novelty introduced is clearly stated in the following subsections.

## 2.1 Newton method

The Newton method [41] provides a good approximation for the root of an objective function. Essentially, the independent variables vector $\boldsymbol{\epsilon}$ of the objective function is iteratively updated from step $k$ to the following $k + 1$ by

$$\boldsymbol{\epsilon}^{(k+1)} = \boldsymbol{\epsilon}^{(k)} + \lambda \boldsymbol{p}^{(k)} \tag{2}$$

where $\lambda$ is the step length, which defines how far the next step moves along the Newton direction $\boldsymbol{p}^{(k)}$. The step length is set in two stages. First, an initial value of 1 is given and it is continuously halved until $\boldsymbol{\epsilon}^{(k+1)}$ satisfies the variable constraints of each problem, specified in the following sections. These constrains may be related, for instance, to the feasible values of density or compositions. Then, an inexact line search is executed to obtain a step length that satisfies the Wolfe conditions[42], which gives an efficient decrease of the objective function.

The Newton direction $\boldsymbol{p}^{(k)}$ is calculated by solving the system of equations:

$$\boldsymbol{H}^{(k)}\boldsymbol{p}^{(k)} = -\boldsymbol{g}^{(k)} \tag{3}$$

where $\boldsymbol{g}$ and $\boldsymbol{H}$ are the gradient and Hessian of the objective function to be minimised. In case the use of successive substitution iterations (SSI) method is needed, the only difference with the Newton method is that the Hessian is equal to the identity matrix $\boldsymbol{I}$.

For the system (3) to have a solution, the Hessian $\boldsymbol{H}$ needs to be positive definite, i.e. its eigenvalues are all positive real numbers. To satisfy this condition, the modified Cholesky factorisation[38] is applied in this study. The modifications introduce symmetric interchanges of rows and columns, via a permutation matrix $\boldsymbol{P}$, and the addition of a non-negative diagonal matrix $\boldsymbol{E}$ which is zero if the Hessian $\boldsymbol{H}$ is positive. Therefore, the system of equations (3) gets transformed, for every iteration step $k$, into:

$$[\boldsymbol{P}(\boldsymbol{H} + \boldsymbol{E})\boldsymbol{P}^T](\boldsymbol{P}\boldsymbol{p}) = -\boldsymbol{P}\boldsymbol{g} \tag{5}$$

Once the positive definiteness of the modified Hessian is satisfied, it is factorised as:

$$\boldsymbol{P}(\boldsymbol{H} + \boldsymbol{E})\boldsymbol{P}^T = \boldsymbol{M}\boldsymbol{M}^T \tag{6}$$

where $\boldsymbol{M}$ is a lower triangular matrix. Finally, the system is solved by performing backward and forward substitution with the triangular matrix, which consists in the following sequence of operations:

1. Solve $\boldsymbol{Mu} = -\boldsymbol{Pg}$ to obtain $\boldsymbol{u}$.
2. Solve $\boldsymbol{M^T}\tilde{\boldsymbol{u}} = \boldsymbol{u}$ to obtain $\tilde{\boldsymbol{u}}$.
3. Calculate the gradient $\boldsymbol{g} = \boldsymbol{P^T}\,\tilde{\boldsymbol{u}}$.

**Convergence criteria**

The Newton method is assumed to have converged whenever one of the following criteria is achieved:

1. The Euclidean norm of the change in the iteration variables $\|\lambda \boldsymbol{p}\|^2$ is less than $10^{-7}$.
2. The Euclidean norm of the gradient $\|\boldsymbol{g}\|^2$ is less than $10^{-10}$.

## 2.2 Stability stage

The stability problem is solved in a similar fashion as that presented by Baker et al. [43]for a mixture at constant temperature *T* and pressure *P*. A homogeneous mixture at a certain temperature *T* is in a stable state if the tangent plane to the Helmholtz free energy surface at composition *z* and density $\rho$ does not intersect the Helmholtz free energy surface at any other point. The stability is tested by purposely dividing the homogeneous mixture in two phases, one of them in an infinitesimal amount and it is referred to as 'trial phase'. For any feasible two-phase mixture, if a decrease in the Helmholtz free energy is not achieved, then the mixture is stable. The so-called tangent plane distance (*TPD*) as function of the density times the composition of the trial phase $\rho' x_i'$ is:

$$TPD(\rho' x_i') = -\frac{P' - P^*}{R_g T} + \sum_{i=1}^{nc} \rho' x_i' (log\, f_i' - log\, f_i^*) \tag{7}$$

where the tildes over the variables indicate those calculated at the trial conditions and the asterisk indicates those calculated at the feed conditions. $R_g$ is the universal gas constant and $f_i$ is the fugacity of

the component *i*. Within the structure of PC-SAFT, it is advisable to write the expression in terms of the residual reduced Helmholtz free energy, having then:

$$P = \left(1 + \rho_m \frac{\partial a^{res}}{\partial \rho_m}\right) k_B T \rho_m \left(10^{10} \frac{\text{Å}}{m}\right)^3 \tag{8}$$

Where $\rho_m$ is the number density of molecules and $k_B$ is the Boltzmann constant. Regarding the fugacity,

$$log\, f_i \quad = log(x_i P \phi_i) \tag{9}$$

Where the logarithm of the fugacity coefficient $\phi$ of the component $i$ is defined as:

$$log\phi_i = \frac{1}{R_g T} \left(\frac{\partial A^r}{\partial N_i}\right)_{T,V,N_s \neq i} - \log Z \tag{10}$$

where $Z$ is the compressibility factor and $A^r$ is the non-reduced Helmholtz free energy. This equation is used for the Peng Robinson EoS following the formulation of Nichita[33]. For PC-SAFT, the original formulation of Gross and Sadowski[1] is used:

$$log\, \phi_i = a^{res} + \rho_m \frac{\partial a^{res}}{\partial \rho_m} + \frac{\partial a^{res}}{\partial x_i} - \sum_{j=1}^{nc} x_j \frac{\partial a^{res}}{\partial x_j} \tag{11}$$

The derivation of the TPD function can be seen in the work of Mikyska and Firoozabadi[44]. The stability is assured if for any feasible solution $\rho' x_i'$ the TPD function is non-negative. Therefore, the problem is reduced to the search of the global minima of the TPD function, subjected to the material constraints:

$$\rho' x_i' > 0 \quad \forall i \tag{12}$$

$$\sum_{i=1}^{nc} \rho' x_i' \leq \rho_{max}(x_i', T) \tag{13}$$

where $\rho_{max}$ refers to the maximum packing fraction at fixed composition $x_i'$ and temperature *T*. For the Newton method, the required gradient is given by:

$$\frac{\partial TPD}{\partial(\rho' x_i)} = log\, f_i' - log\, f_i^* \tag{14}$$

Nichita [45] studied alternatives to use as iteration variables such as $\log(\rho' x_i')$ and $\alpha_i = 2\sqrt{\rho' x_i'}$, in a similar manner as shown by Michelsen[28]. His study concluded that the $\alpha_i$ ensured the most robust and

fast convergence for the stability problem and it is the one used in this work. For this case, the gradient is:

$$\frac{\partial TPD}{\partial \alpha_i} = \sqrt{\rho' x_i}(\log f_i' - \log f_i^*) \tag{15}$$

and the Hessian is:

$$\frac{\partial TPD}{\partial \alpha_i \, \partial \alpha_j} = \delta_{ij} + \sqrt{\rho' x_i}\sqrt{\rho' x_j}\left[\frac{\partial \log f_i}{\partial n_j} - \frac{\delta_{ij}}{\rho' x_i}\right] \tag{16}$$

In order to avoid unnecessary iterations when the Newton is converging to a trivial solution, i.e. *TPD* = 0, in this work another stopping criterion is used, also first introduced but for the TPN case by Michelsen[28]. At every iteration the convergence variable *r* is checked:

$$r = \frac{2\,TPD^{(k)}}{\sum_{i=1}^{nc}(\rho' x_i - \rho z_i)\left(\log f_i' - \log f_i^*\right)} \tag{17}$$

which tends to 1 as the method converges to the trivial solution. Therefore, the iterations are stopped if $|r - 1| < 0.2$ and $TPD^{(k)} < 10^{-3}$.

## 2.3 Initialisation

The stability stage needs an initial condition to start the iterative process. Tipically, Wilson's correlation [46] is used to guess the initial equilibrium constants $K_i$:

$$K_i = \frac{P_{c,i}}{P}\exp\left[5.37(1+\omega_i)\left(1 - \frac{T_{c,i}}{T}\right)\right] \tag{18}$$

where for every component *i*, $P_{c,i}$ and $T_{c,i}$ are the critical pressure and temperature and $\omega_i$ is the acentric factor. These three values are used in most cubic EoS and are widely available in the literature, but not in PC-SAFT EoS. However, the exact critical values specific for the PC-SAFT EoS can be calculated following a published algorithm[47], which comprises an iterative process in order to verify the three critical specifications:

$$P(T_c, \rho_c) - P_c = 0 \tag{19}$$

$$\frac{\partial P}{\partial \rho} = 0 \text{ at } (T_c, \rho_c) \tag{20}$$

$$\frac{\partial^2 P}{\partial \rho^2} = 0 \text{ at } (T_c, \rho_c) \tag{21}$$

Unlike for the PT-multiphase problem, the pressure of the mixture is unknown a-priori for VT specifications, so a different strategy must be used, as the one used by Nichita[45]. According to Raoult's law:

$$K_i = \frac{P_{sat,i}(T)}{P} \tag{22}$$

where $P_{sat,i}(T)$ is the saturation pressure of the component *i* at a temperature *T*. From this law, follows that $P_{sat,i}(T) = P$ when $K_i = 1$, therefore from eq. (13) it follows:

$$P_{sat,i}(T) = P_{c,i} \exp\left[5.37(1+\omega_i)\left(1-\frac{T_{c,i}}{T}\right)\right] \tag{23}$$

The strategy for the initial composition of the trial phase is slightly different if it is considered to be vapor-like or liquid-like. Michelsen [28] proposed the initial composition of the trial phase, for both cases, to be:

$$x_i^{v(0)} = z_i K_i^{(0)} \quad \text{and} \quad x_i^{l(0)} = \frac{1}{z_i K_i^{(0)}} \tag{24}$$

which, using Raoul's law (14) transform to:

$$x_i^{v(0)} = z_i \frac{P_{sat,i}(T)}{P^{v(0)}} \quad \text{and} \quad x_i^{l(0)} = \frac{z_i}{P_{sat,i}(T)} P^{l(0)} \tag{25}$$

where the initial pressures $P^{v(0)}$ and is $P^{l(0)}$ are first taken as that given by the EoS for the single phase system at $T$, $\rho$ and composition $\boldsymbol{z}$. If the calculated pressure is negative, Mikyska and Firoozabadi [44] estimated them as:

$$P^{v(0)} = \sum_{i=1}^{nc} z_i P_{sat,i}(T) \quad \text{and} \quad P^{l(0)} = \sum_{i=1}^{nc} \frac{P_{sat,i}(T)}{z_i} \tag{26}$$

The initial density of the trial phase is then calculated iteratively using the EoS for both initial compositions $x_i^{v(0)}$ and $x_i^{l(0)}$ at fixed temperature $T$ and at the corresponding initial pressures $P^{v(0)}$ and

$P^{l(0)}$. As there may be two densities for every composition and pressure, there can be up to 4 initial estimates; all the initial estimates are used in the stability stage.

## 2.4 Initial Phase splitting

In case the mixture is found to be unstable, an initial splitting of the homogeneous phase is executed. From the stability analysis, the composition and density of the trial phase are fixed to $\rho'$ and $x_i'$. With variations with respect to the method shown by Jindrova and Mikyska[32], the initial density and composition of the second phase, i.e. $\rho''$ and $x_i''$, are estimated in terms of the molar fraction of the trial phase over the feed, $\beta = N'/N^*$, from the material and volume constraints:

$$\beta x_i' + (1-\beta)x_i'' = z_i \tag{27}$$

$$\beta \frac{1}{\rho'} + (1-\beta)\frac{1}{\rho''} = \frac{1}{\rho} \tag{28}$$

The initial amount of each phase is estimated in the following way:

1. An arbitrary initial trial molar fraction β is chosen. In two phase systems, $\beta \in (0,1)$, thus the chosen initial value in this work is 0.99.
2. The composition and density of the second phase are calculated from the material and volume constraints (19) (20) by:

$$x_i'' = \frac{z_i - \beta x_i'}{1-\beta} \tag{29}$$

and

$$\rho'' = \frac{1-\beta}{\frac{1}{\rho} - \beta\frac{1}{\rho'}} \tag{30}$$

3. The density of the second phase is checked to be lower than that given by the maximum packing fraction

$$\rho'' < \rho_{max}(x_i'', T) \tag{31}$$

If not, a new lower molar fraction value is assumed (i.e. halving the previous value), and the algorithm returns to step 2.

4. The variation in the Helmholtz free energy is calculated by:

$$\Delta A = A^{2\,phase} - A^{*} = \left(A'(\boldsymbol{x}', \rho', T) + A''(\boldsymbol{x}'', \rho'', T)\right) - A^{*} \quad (32)$$

5. It is checked whether $\Delta A < 0$, meaning that the current phase split produces a decrease in the Helmholtz free energy. If $\Delta A \geq 0$ the molar fraction is halved and step 2 is repeated. If $\Delta A < 0$ the process is stopped, and the flash stage begins. The phase with the highest density is considered to be the liquid phase (*l*) and the other one the vapor phase (*v*).

## 2.5 Flash stage

Following the initial phase splitting, the flash stage calculates the amount and compositions of both phases in equilibrium, in addition to the final equilibrium pressure. This calculation is done via the minimisation of the variation of the Helmholtz free energy, as in equation 24. Depending on the iteration variables, two methodologies have been tested. Firstly, the one described by Jindrova and Mikyska [39] uses the number of moles in both phases and the phase volumes. Secondly, the one described by Nichita [33] uses the natural logarithm of the equilibrium constants. The two methods have been coupled with the PC-SAFT framework and the derivatives needed can be found in the Supplementary Information.

### Number of moles and volume as iteration variables

When using the number of moles and the volume of both phases, per mole of feed, the problem comprises (2 *nc*)+2 iteration variables $n_1^v, \dots, n_{nc}^v, V^v, n_1^l, \dots, n_{nc}^l, V^l$. However, because of the material and volume balances:

$$n_i^v + n_i^l = z_i \tag{33}$$

$$V^v + V^l = \frac{1}{\rho} \tag{34}$$

the variables of one phase are dependent on those of the other phase. Therefore, as described by Jindrova and Mikyska[39], it is possible to solve a reduced system in terms of the *nc*+1 vapor variables. For the reduced problem, the gradient of the system is given by:

$$g_i = \frac{\partial \Delta A}{\partial n_i^v} = \frac{\log f_i^v - \log f_i^l}{\sqrt{2}} \quad \text{for} \quad i = 1, nc \tag{35}$$

$$g_{nc+1} = \frac{\partial \Delta A}{\partial V^v} = -\frac{P^v - P^l}{\sqrt{2} R_g T} \tag{36}$$

and the Hessian:

$$\boldsymbol{H} = 1/2\begin{pmatrix} & \boldsymbol{B} & & \vdots & \boldsymbol{C} \\ & & & \vdots & \\ \cdots & \cdots & \cdots & \vdots & \cdots \\ & \boldsymbol{C}^T & & \vdots & D \end{pmatrix} \tag{37}$$

Where

$$B_{ij} = \frac{\partial \log f_i^v}{\partial n_j^v} + \frac{\partial \log f_i^l}{\partial n_j^l} \tag{38}$$

$$C_i = -\frac{\frac{\partial P^v}{\partial n_i^v} + \frac{\partial P^l}{\partial n_i^l}}{R_g T} \tag{39}$$

$$D = -\frac{\frac{\partial P^v}{\partial V^v} + \frac{\partial P^l}{\partial V^l}}{R_g T} \tag{40}$$

In order to obtain the variation of the variables for both phases, the Newton direction *p* is transformed back into the full (2 *nc*)+2 dimension premultiplicating by the reducing matrix *Z:*

$$\boldsymbol{Z} = \frac{1}{\sqrt{2}}\begin{pmatrix} I_{nc+1} \\ -I_{nc+1} \end{pmatrix} \tag{41}$$

Finally, the composition and density of both phases are calculated by first obtaining the vapor mole fraction $\beta = \sum_{i=1}^{nc} n_i^v$ and then:

$$x_i^v = \frac{n_i^v}{\beta} \quad \text{and} \quad x_i^l = \frac{n_i^l}{1-\beta} \tag{42}$$

$$\rho^v = \frac{\beta}{V^v} \quad \text{and} \quad \rho^l = \frac{1-\beta}{V^l} \tag{43}$$

Following the work of Paterson et al.[34], the effect of initial Successive Substitution Iterations (SSI)during the flash stage were tested. However, no improvement was observed and on average more iterations were needed to reach convergence.

**Logarithm of equilibrium constants $\log K_i$ as iteration variables**

The use of the logarithms of equilibrium constants, $\log K_i = \log(x_i^v / x_i^l)$, as iteration variables in the flash problem is one of the most used methods when the multiphase problem is defined in terms of pressure and temperature. Nichita [33] applied it to the VT-Flash problem by decoupling the pressure

equality condition $P^v(x_i^v, \rho^v, T) = P^l(x_i^l, \rho^l, T) = P^{eq}$, which is calculated at every iteration step. Therefore, the iteration variables are reduced to the $nc$ components defining $log\ \boldsymbol{K}$. Then, at every step the Rachford-Rice equation is solved to obtain the vapor mole fraction β using the Newton-Raphson method:

$$\sum_{i=1}^{nc} \frac{z_i(K_i-1)}{1+\beta(K_i-1)} = 0 \tag{44}$$

Which allows to obtain the molar fractions of both phases for every iteration $k$ by:

$$x_i^l = \frac{z_i}{1+\beta(K_i-1)} \tag{45}$$

and

$$x_i^v = K_i x_i^l \tag{46}$$

Then, the equilibrium pressure $P^{eq}$ is calculated iteratively by solving the volume distribution equation:

$$\beta \frac{1}{\rho^v(x_i^v, P^{eq}, T)} + (1-\beta)\frac{1}{\rho^l(x_i^l, P^{eq}, T)} = \frac{1}{\rho} \tag{47}$$

When calculating the density at certain pressure, many roots may be encountered. In such a case, the density giving the least Gibbs free energy is chosen. The iterative method chosen is that of Brent[48]. The gradient in this case reads:

$$\frac{\partial \Delta A}{\partial \log K_i} = \log f_i^v - \log f_i^l \tag{48}$$

and the Hessian:

$$H_{ij} = \frac{\partial\ log\, K_i}{\partial\, N_j^v} + \frac{\partial\ log\, f_i^v}{\partial\, N_j^v} + \frac{\partial\ log\, f_i^l}{\partial\, N_j^l} + \frac{1}{R_g\, T} \frac{\left(\frac{\partial\, P^v}{\partial\, N_i^v} + \frac{\partial\, P^l}{\partial\, N_i^l}\right)\left(\frac{\partial\, P^v}{\partial\, N_j^v} + \frac{\partial\, P^l}{\partial\, N_j^l}\right)}{\frac{\partial\, P^v}{\partial\, V^v} + \frac{\partial\, P^l}{\partial\, V^l}} \tag{49}$$

As proposed in the original paper of Nichita[33], a first iteration using the SSI method is applied.

# 3 Results and Discussion

In this section, results for the VLE problem using composition, density and temperature are shown for a set of seven cases. Case 1 is a single component Diesel surrogate, (n-dodecane) widely used in the Diesel industry; this case will show the performance of the algorithm for single components where the PT FLASH fails. Cases 2 and 3 are binary mixtures, typically used as benchmark cases for testing multiphase equilibrium algorithms[31]. The composition for Case 2 is 0.547413 methane and 0.452587 pentane, while for Case 3 is 0.547413 carbon dioxide and 0.452587 decane. Case 4 is another binary mixture used in the widely used database of the so-called 'Spray A'[49], 0.3 nitrogen and 0.7 dodecane. Case 5 is a four-component mixture, also widely used for testing of multiphase algorithms[31], composed of 0.2463 nitrogen, 0.2208 methane, 0.2208 propane and 0.3121 decane. Case 6 is a hydrocarbon eight-component mixture created also as a Diesel fuel surrogate[50], composed of 0.202 octadecane, 0.027 hexadecane, 0.292 heptamethylnonane, 0.144 1-methylnaphthalene, 0.154 tetralin, 0.055 trans-decalin, 0.051 butylcyclohexane and 0.075 1,2,4-trimethylbenzene. Finally, case 7 explores the application of the presented method to a multi-component mixture consisting of 50 different hydrocarbons, with equally distributed composition ranging from methane to octadecane. The complete set of hydrocarbons is given in the Supplementary Information. Cases 3 and 4 are validated against experiments, apart from an additional synthetic mixture of 6 components, commonly named Y8[51]. For all cases, the EoS parameters and binary interaction parameters are given in the Supplementary Information. Table 1 shows the density-temperature grids studied for each case, apart from the number of total points tested with the algorithms.

A summary of the iterations needed for convergence for every stage and flash methodologies used in this work can be found in Table 2. The average values are calculated as the sum of the iterations needed until convergence for the whole domain and then divided for the number of points studied. As seen in the first row, the stability analysis grows with the number the components of the mixture. While for a single component (Case 1), the number of iterations needed for convergence in stability is around 4, for binary mixtures (Cases 2-4), it increases to around 7. For the 4 components mixture (Case 5), the

number of stability iterations needed are not much affected with respect to the binary mixtures. For the eight-component hydrocarbon mixture (Case 6), the average number of iterations needed grows around 50%. Finally, for the 50-component mixture (Case 7), the number of iterations is higher but close to the previous case.

| Case | $nc$ | $T$(K) window | $T$(K) no. points | $\rho$ (Kmol/m$^3$) window | $\rho$ no. points | Total no. points |
|---|---|---|---|---|---|---|
| 1 | 1 | [280-700] | 400 | [0.001-5] | 400 | 160000 |
| 2 | 2 | [320-430] | 110 | [0.001-12] | 1200 | 132000 |
| 3 | 2 | [250-600] | 350 | [0.001-9] | 900 | 315000 |
| 4 | 2 | [250-650] | 400 | [0.001-10] | 900 | 360000 |
| 5 | 4 | [250-600] | 350 | [0.001-12] | 1200 | 420000 |
| 6 | 8 | [300-750] | 450 | [0.001-4.5] | 450 | 202500 |
| 7 | 50 | [300-650] | 400 | [0.001-6] | 400 | 160000 |

Table 1: Density-Temperature window and total number of points.

A case dependant result is found for the flash stage. For the NVL method (second row of Table 2), the binary mixture of Case 2 is the one with the lower number of flash iterations needed, followed by the single component Case 1 and the other two binary mixture Cases 3 and 4. A substantial increase is found for the 4-component mixture, which almost triples the iterations needed for the binary mixtures. Although doubling the number of components in Case 6, for the 8-component the flash iterations gets reduced by 10 for the conditions to converge. Finally, the 50-component mixture shows a doubled number of iterations with respect to Case 6, needing on average around 30 iterations until convergence during the flash stage.

In the case of the lnK method (third row on Table 2), the number of iterations is significantly reduced by more than 40% with respect to the NVL method. However, as explained in the methodology section for the lnK independent variables, this method suffers from the same limitation of the PT-Flash problem

and it can't be used for single components and mixtures of similar components, as Cases 1 and 6. Regarding the rest of cases, Case 2 is the one with the least iterations needed (up to 4), followed by the other binary mixtures Cases 4 and 3. For Case 5, the 4-component mixture needs between 3 and 4 times more iterations than for the binary mixtures. For the 50-component surrogate, the difference between the methods gets reduced to only 2 iterations less than those needed for the NVL-VLE algorithm.

| | Case 1 | Case 2 | Case 3 | Case 4 | Case 5 | Case 6 | Case 7 |
|---|---|---|---|---|---|---|---|
| Stability | 3.93 | 7.63 | 6.26 | 6.87 | 11.25 | 15.31 | 17.82 |
| Flash (NVL) | 7.24 | 6.26 | 9.05 | 9.21 | 26.82 | 16.20 | 30.80 |
| Flash (lnK) | - | 3.99 | 5.32 | 4.24 | 15.12 | - | 28.33 |

Table 2: Average number of iterations needed for convergence using every method studied here for both the stability and flash algorithms.

Table 3 shows the average total convergence time, i.e. both stability and flash stages, for any $\rho$ and $T$ conditions, in ms. The CPU used during this study was an Intel(R) Xeon(R) CPU E5-2690 v3 at 2.60GHz and a memory of 128GB of RAM. From the number of iterations, it would seem clear that the lnK method was the best one to be used in processes needing fast but reliable calculations, such as those needed in CFD simulations. However, the time needed for convergence clearly points in the opposite way, as the lnK method lasts a minimum of 20 times longer than the time needed for convergence with the NVL. This difference in computational time is caused during the calculation of density in the pressure equality condition, as it needs to be obtained iteratively, while NVL only satisfies it once convergence is reached. For the single component Case 1, the NVL method needed 0.6 ms, while no results could be obtained for the lnK method as it fails. For the binary mixtures (Cases 2-4), around 1 ms was needed for the NVL method against the 20-25ms for the lnK. The computational time needed for the 4-component mixture of Case 5 was around 5ms for the NVL method and 135ms for the lnK method (25 times longer). Case 6 needed 15.6 ms with NVL while the lnK method failed to converge to the correct solution whenever the phase transition was isobaric-isothermal. For the 50-components mixture of Case 7, each complete VLE calculation took close to 2 seconds, while for the lnK flash procedure it took 10 times longer. Therefore, the NVL method is chosen in the following sections.

| Flash strategy | Case 1 | Case 2 | Case 3 | Case 4 | Case 5 | Case 6 | Case 7 |
|---|---|---|---|---|---|---|---|

| | | | | | | | |
|---|---|---|---|---|---|---|---|
| NVL | 0.68965 | 1.0782 | 1.1203 | 0.77236 | 7.2450 | 35.401 | 1,955 |
| lnK | - | 19.933 | 24.141 | 23.72 | 135.48 | - | 18,378 |

Table 3: Average time, in ms, per case needed for convergence using both flash methods studied here.

In the following subsections, results from using NVL iterations are shown regarding the pressure field, vapor volume fraction and number of flash iterations for convergence. Finally, results are validated against experimental VLE data. All the calculation data can be found in the supplementary information.

## 3.1 Pressure Field

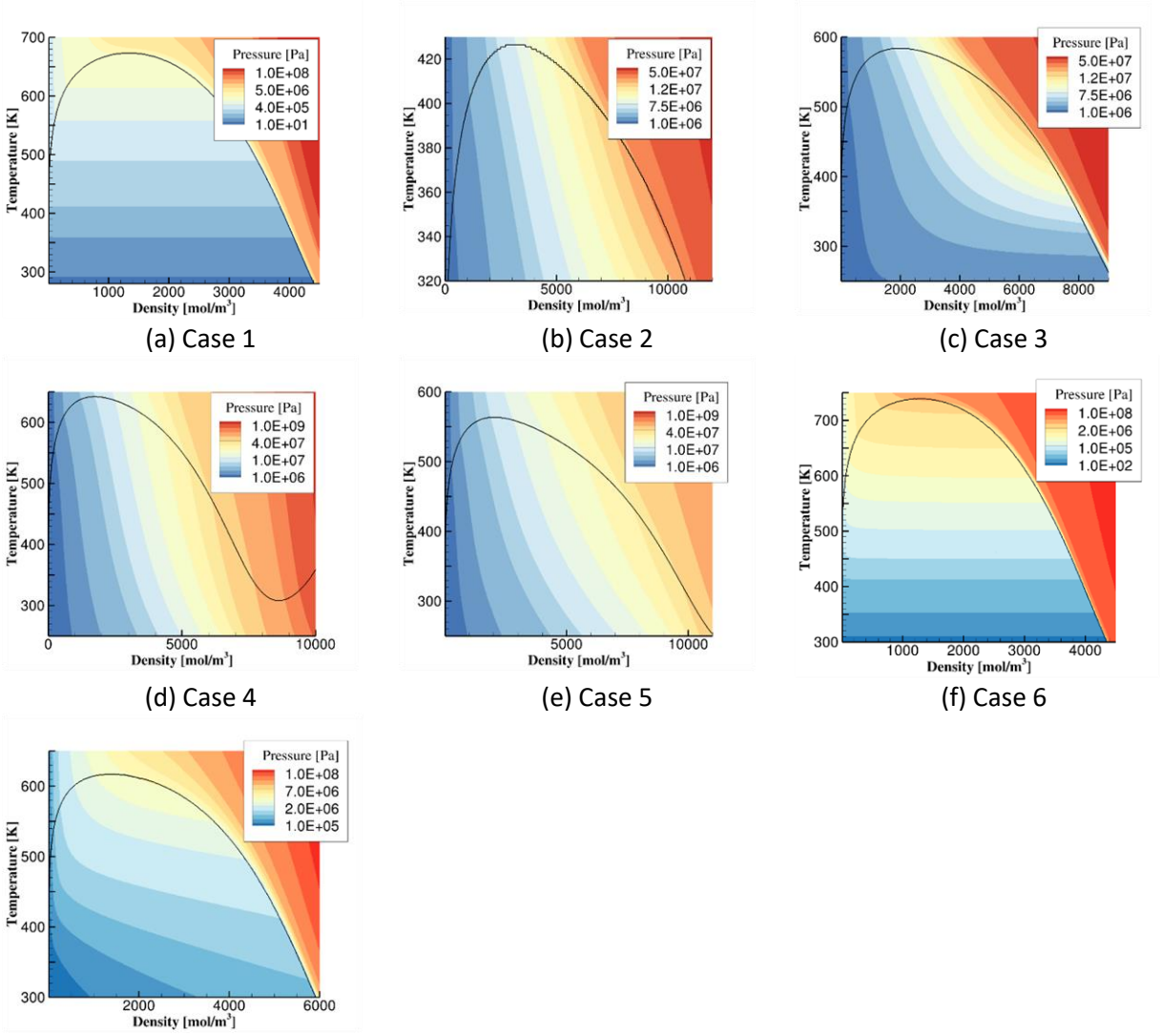


Figure 1. Pressure field for all cases studied in the paper, the black curve draws the saturation line. The colour scale is unique for every figure.

Figure 1 shows the pressure field for every case, marking with a black curve the saturation line. Depending on the components and composition, the pressure field varies significantly. Cases 1 and 6, those which are meant to model Diesel fuel, show similar horizontal isobaric lines when in the VLE region, where the PT-VLE algorithm is known to fail. Case 1 shows isobaric-isothermal phase transition by definition, as it is a single component. Case 6, the 8-component mixture, shows a similar trend due to the similarity between the components, although the small differences among them can be seen close to the dew curve, where the isobars bend upwards. Cases 2, 4 and 5 show isobars with significant slope which isobaric vapor-liquid transition comes with a massive decrease in temperature, typical of mixtures

exhibiting extremely different phase transition properties. For instance, from Case 2 the critical temperature of pentane is close to 2.5 times than that of methane, while more obviously in Case 4 the critical temperature of dodecane is more than 5 times higher than that of dodecane. Case 3 shows an intermediate field between Cases 1 and 2, where while at high temperatures the slope is sufficiently pronounced, at low temperatures and high densities the isobars become progressively flat, where the PT-VLE problem is expected to start failing. Regarding the 50-component hydrocarbon mixture, the isobars show significant slope as there are both very light and very heavy hydrocarbons, for instance methane and octadecane.

## 3.2 Vapor volume Fraction Field

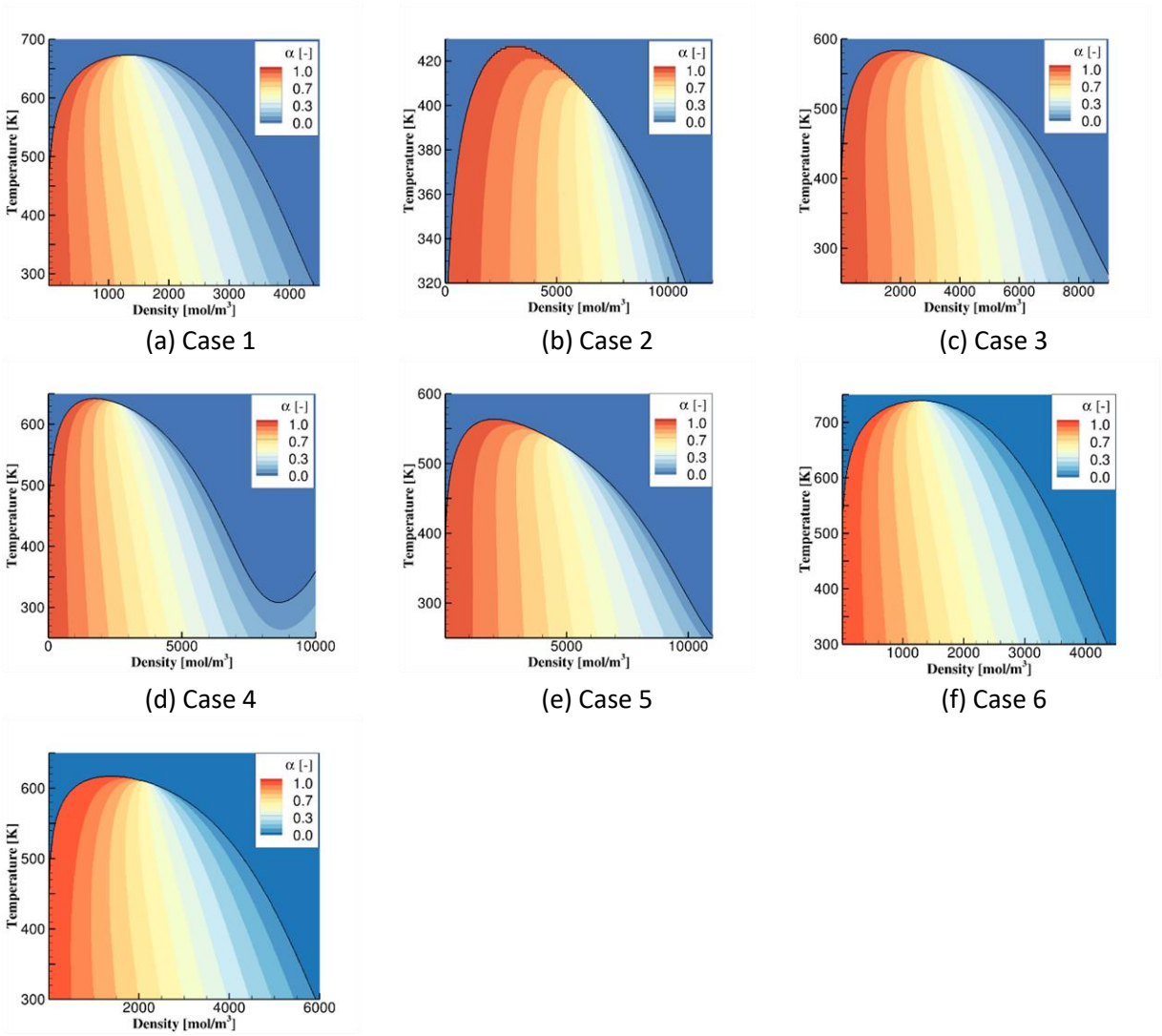


(a) Case 1 (b) Case 2 (c) Case 3

(d) Case 4 (e) Case 5 (f) Case 6

(g) Case 7

Figure 2. Vapor volume fraction field for all cases studied in the paper, the black curve draws the saturation line. The colour scale is the same on every figure.

Figure 2 shows the vapor volume fraction field for every case, marking with a black curve the saturation line. Cases 1 and 6 show the typical vapor volume fraction field for every single component, where the isolines converge at the critical point, being in this case the maximum temperature and pressure at which a two-phase state can be found. On the rest of cases, the critical point is not located on the maximum two-phase temperature or pressure, but on a lower value. This phenomenon gives rise to the retrograde vaporisation[52], which accounts for the anomalous isothermal vaporisation of the mixture when the pressure is increased. Case 4, in addition, shows at 320K a liquid-liquid critical point,

where the equilibrium pressure is higher than 100MPa, clearly seen on the change in curvature of the saturation curve.

## 3.3 Flash iterations until convergence

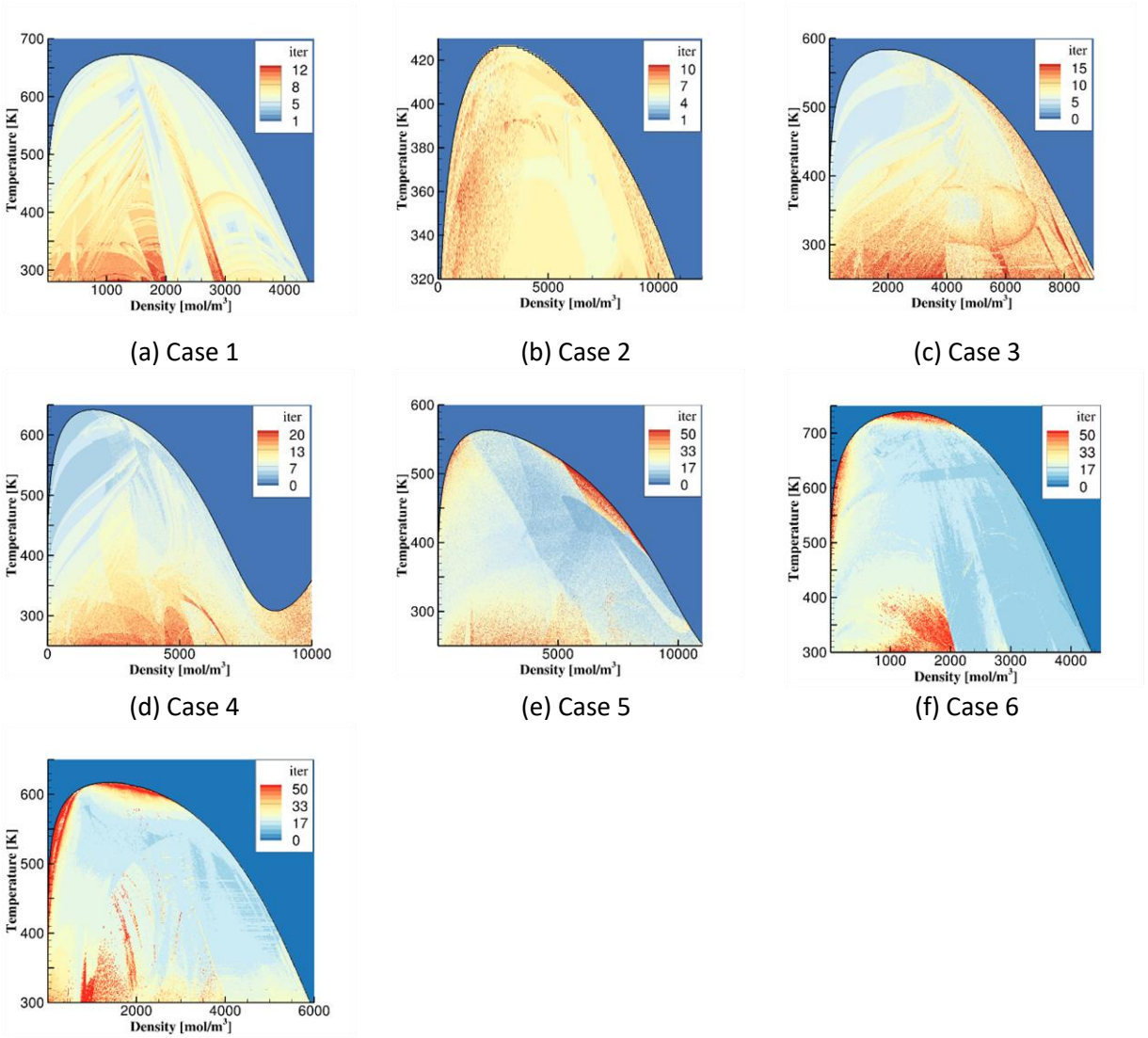


(a) Case 1 (b) Case 2 (c) Case 3

(d) Case 4 (e) Case 5 (f) Case 6

(g) Case 7

Figure 3. Flash iterations field for all cases studied in the paper, the black curve draws the saturation line. The colour scale is unique for every figure.

Figure 3 shows the number of flash iterations needed for convergence using the NVL-algorithm for every case, marking with a black curve the saturation line. Case 1 shows a reasonably homogeneous distribution, with maximum number of iterations of 10 at low temperatures and intermediate densities. The distribution of Case 2 iterations is as homogeneous as in Case 1, with a maximum iteration number of 10. For Case 3, the highest numbers are localised at temperatures lower than 350K and close to the bubble-point curve, where the number of iterations reach 15. Regarding Case 4, the higher number of iterations are found at temperatures lower than 350K and at densities higher than 9,000mol/m$^3$, where the calculated equilibrium pressure reaches 1,000MPa. For the 4-component mixture in Case 5, more

than 50 iterations are needed along to the bubble point curve at high temperatures. High number of iterations are also observed for temperatures lower than 300K and close to the dew-point curve at high temperatures. Overall, at high temperatures the phase change needs a particularly high number of iterations for convergence. The 8-component surrogate in Case 6 the maximum number of iterations, which may reach 100, are found close to the critical point and at high temperatures close to the dew-point curve. For the 50-component hydrocarbon mixture, the number of iterations grow considerably compared with the previous cases, where the threshold of 150 iterations is reached again at the critical point and the dew curve, in addition to localised high number of iterations at 1,000mol/$m^3$ and temperatures lower than 350K.

## 3.4 Performance comparison against Peng Robinson EoS

The performance of the algorithm can be influenced significantly by the chosen equation of state, as every iteration needs the calculation of many properties and its derivatives for the two phases. The use of PC-SAFT EoS has been already reported to increase the computational time needed for a single equilibrium calculation with respect to Peng Robinson[53]. Previous works, using a PT-VLE calculation, have obtained differences in CPU time of 2-3 times between the Peng Robinson EoS and PC-SAFT EoS[40] for a variety of mixtures. For some mixtures, even, the computational time was found smaller for the original PC-SAFT than for the cubic EoS. However, von Solms[40] estimated that the CPU time needed for the calculation of all the derivatives involved in the PT-VLE was 4-5 times higher than for the SRK EoS, using the simplified PC-SAFT for a mixture of 15 components. The simplified PC-SAFT is known to be significantly more efficient in VLE calculations as some of the terms of the original version become composition-independent. Therefore, the difference between cubic EoS and the PC-SAFT is expected to be higher than 4-5 times, even if the number of function evaluations is similar.

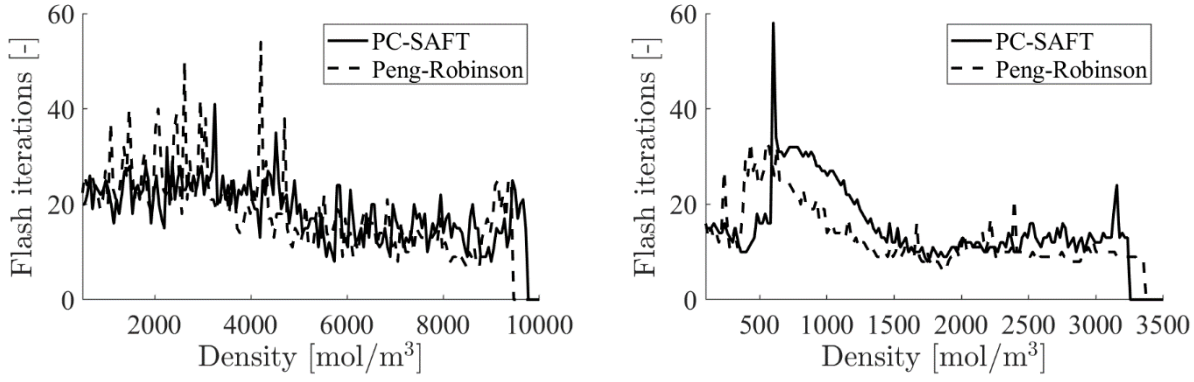


(a) (b)

Figure 4. Flash iterations needed for Cases 5 and 6 at 300K using Peng-Robinson and PC-SAFT as Equations of State at 300K.

Figure 4 shows two performance comparisons for Cases 5 (4 component mixture) and 6 (8 component mixture) regarding the iterations needed for calculating the equilibrium at 300K for a range of densities, using both Peng Robinson and PC-SAFT EoS. Flash iterations are both initialized from a previous stability analysis. As shown, for the 4-component mixture the iterations needed are quite similar for both

Equations of State, apart from particular conditions at which the cubic equation seems to spike. Overall, the iterations needed at lower densities than 5000mol/m3 are higher than those at higher densities. For the 8-component surrogate, the number of iterations needed at low densities are significantly higher for PC-SAFT, although at densities higher than 1500mol/m3 the convergence is achieved in a similar number of iterations.

| EoS | Case 1 | Case 2 | Case 3 | Case 4 | Case 5 | Case 6 | Case 7 |
|---|---|---|---|---|---|---|---|
| PC-SAFT | 629.79 | 1340.6 | 1143.8 | 1059.4 | 1878.1 | 13996 | 363270 |
| Peng Robinson | 156.25 | 182.62 | 191.98 | 210.94 | 250.31 | 937.53 | 10332 |
| Ratio | 4.03 | 7.34 | 5.96 | 5.02 | 7.5 | 14.9 | 35.16 |

Table 4: Computational time in μs, per single VLE calculation, needed for all cases using Peng Robinson and PC-SAFT. The last row shows the ratio between both CPU times.

Table 4 shows the computational time, per VLE calculation, needed for all cases using both Peng Robinson and PC-SAFT EoS. Results indicate a significant difference between both EoS, which increases with the number of components. While for a single component the CPU time for PC-SAFT is about 4 times higher than for Peng-Robinson, for two components it grows to about 6 and up to 15 for the 8-component surrogate of case 6. An extreme case is seen for case 7, where the computational time needed to calculate the VLE for a 50-component mixture increases to 35. These differences can be explained due to the high dependence on composition of the PC-SAFT EoS, which increases the number of calculations needed for the derivatives exponentially. The reader may acknowledge the extent of the derivations in the complete formulation of the algorithm found in the Supplementary Information. This can be also seen in Table 5, where the computational time per single calculation of the derivatives is shown. The range in temperature and density per case is the same as in previous chapters. As seen, the difference between the CPU time of Peng Robinson and PC-SAFT grows with the number of components in a similar fashion than for the complete VLE calculations. Discrepancies between the single EoS and complete VLE calculations can be explained because of differences in the number of iterations needed for the convergence, which is not necessarily the same, although similar as already seen in Figure 4.

| EoS | Case 1 | Case 2 | Case 3 | Case 4 | Case 5 | Case 6 | Case 7 |
|---|---|---|---|---|---|---|---|
| PC-SAFT | 8.844 | 13.37 | 13.70 | 14.66 | 31.20 | 100.0 | 25380 |
| Peng Robinson | 1.800 | 2.323 | 2.341 | 2.342 | 3.421 | 7.046 | 58.75 |
| Ratio | 4.91 | 5.76 | 5.84 | 6.25 | 9.12 | 14.19 | 43.2 |

530 Table 5: Computational time in μs, per single calculation of all the needed derivatives, for all cases using
531 Peng Robinson and PC-SAFT. The last row shows the ratio between both CPU times.

532

533 These results show why when computational power is the main restriction in simulations, past works
534 tend to choose the Peng-Robinson over more accurate EoS such as the PC-SAFT. For instance, in
535 Computational Fluid Dynamics, equilibrium calculations may be needed in more than 1 million cells per
536 timestep, making the EoS choice the main decision criterion regarding the trade-off between accuracy
537 and computational efficiency.

## 3.5 Validation against experiments

Figure 6 shows validation cases to assess the accuracy of the model when compared to experimental data. The data was collected and compared for Case 2[54], Case 4 [55] and the Y8 synthetic mixture[51]. The Y8 mixture is composed of 6 components with composition: 0.8097 methane, 0.0566 ethane, 0.0306 propane, 0.0457 n-pentane, 0.0330 n-heptane and 0.0244 n-decane. The binary interaction parameters were set to 0 for the Y8 mixture. As it can be seen, there exists good agreement for every case using the corresponding binary interaction parameters. The first two figures show the typical binary phase diagram at different constant temperatures, while the first figure shows the equilibrium constants for every component in the mixture at fixed temperature.

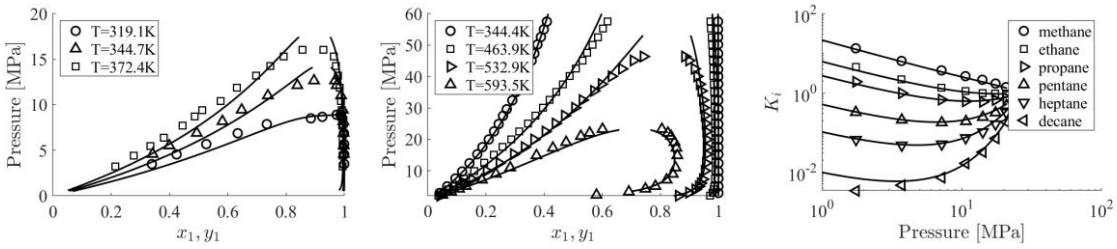


(a) (b) (c)

Figure 6: Predicted vapor-liquid equilibrium compared with experimental data for (a) Case 2, (b) Case 4 and (c) the Y8 mixture [37].

Table 5 shows the Average Absolute Deviation (AAD [%]) of the calculations with respect to the experimental values for the above cases and it is defined as:

$$AAD[\%] = \frac{100}{N_p}\sum_{i}^{N_p}\left|\frac{(x_i, y_i)^{exp} - (x_i, y_i)^{calc}}{(x_i, y_i)^{exp}}\right| \quad (50)$$

Where $N_p$ is the number of compared experimental data points.

| | Case 2 | Case 4 | Y8 Mixture |
|---|---|---|---|
| $AAD[\%]$ | 2.7901 | 0.9281 | 3.6289 |

Table 5: Average Absolute Deviation (AAD [%]) of the three cases shown in Figure 6.

As observed in the table, the agreement with experiments is good even for the 6-component mixture, where the average deviation is lower than 4%. However, it is necessary to notice that this agreement is significantly dependent on the binary interaction parameter $k_{ij}$ which is obtained by fitting with experimental VLE data.

# 4 Conclusions

In this study, the PC-SAFT EoS was used for Vapor Equilibrium calculation at specified composition, density and temperature. The presented algorithm was tested on several cases of both single and multicomponent substances. The calculation utilised the Newton iterations to reach the global minimum of the Helmholtz free energy in two stages, namely stability analysis and flash. As a result, the pressure of the fluid and the compositions of both the liquid and vapor phases were calculated. The reliability of two different methods for the flash stage, one based in number of moles and volume (NVL) and another based in the logarithm of the equilibrium constants (lnK), were evaluated in terms of both iterations and computer time needed to reach convergence.

Results showed that although the lnK method needs less iterations until convergence, the total computational time needed is considerably longer. This difference in computational time is caused during the calculation of density in the pressure equality condition, as it needs to be satisfied iteratively. The NVL method does not need to satisfy this condition at every iteration, therefore no inner iterative loops are needed, and faster convergence was obtained. Moreover, the lnK method cannot be used for single components, as its value is unity during all iterations, and it fails continuously for mixtures with similar components, as the 8-component Diesel surrogate studied in Case 6. A performance comparison was obtained against the Peng-Robinson EoS, showing a substantial decrease in computational time when using the cubic compared to the molecular based EoS. Validation against experiments show good agreement of the numerical model.

Future work should be headed towards more complex mixtures, resourcing to the latest applications of PC-SAFT introducing associating[56], multipolar [57 58] and/or aqueous ionic liquid solutions[59], as the accuracy of this molecular-based EoS is of great value for academic and industrial applications.

# 5 Acknowledgements

This project has received funding from the European Union Horizon-2020 Research and Innovation Programme. Grant Agreement No 675528.

The authors would like to thank the invaluable help of Dr. Mikyška's group, particularly Tomáš Smejkal, for sharing their VLE data and continuous assistance for the completion of this article.

# 6 Nomenclature

| | |
|---|---|
| $A$ | Helmholtz free energy |
| $\boldsymbol{z}$ | pressure |
| $\rho$ | molar density |
| $T$ | temperature |
| $\boldsymbol{E}$ | modified Cholesky diagonal matrix |
| $\boldsymbol{P}$ | permutation matrix |
| $P$ | pressure |
| $\boldsymbol{p}$ | search direction |
| $\boldsymbol{M}$ | Cholesky lower triangular matrix |
| $\boldsymbol{B}$ | Hessian submatrix |
| $\boldsymbol{C}$ | Hessian submatrix |
| $D$ | Hessian submatrix |
| $\boldsymbol{g}$ | gradient vector |
| $\boldsymbol{H}$ | Hessian matrix |
| $\boldsymbol{I}$ | identity matrix |
| $R_g$ | universal gas constant |
| $x_i$ | mole fraction of component $i$ in a phase |
| $z_i$ | mole fraction of component $i$ in the feed |
| $\boldsymbol{Z}$ | reducing matrix |
| $nc$ | number of components |
| $n_i$ | number of moles of component $i$ |
| $f_i$ | fugacity of component $i$ |
| $m$ | number of segments |
| $k_B$ | Boltzmann constant |
| $K_i$ | equilibrium constant |
| $\tilde{\boldsymbol{u}}$ | intermediate Cholesky vector |
| $\boldsymbol{u}$ | intermediate Cholesky vector |
| $V$ | volume |
| $TPD$ | Tangent Plane Distance |

Greek letters

| | |
|---|---|
| $\alpha$ | transformed stability variables |
| $\sigma$ | segment diameter |
| $\delta_{ij}$ | Kronecker delta |
| $\lambda$ | step length |
| $\epsilon$ | energy parameter |
| $\boldsymbol{\epsilon}$ | variables vector |
| $\omega$ | acentric factor |
| $\beta$ | Vapor fraction |

Subscripts

| | |
|---|---|
| $i, j$ | component index |
| $c$ | critical property |
| $sat$ | saturation |
| $max$ | maximum |

Superscripts

| | |
|---|---|
| $*$ | feed property |
| $v$ | vapor phase |
| $l$ | liquid phase |
| $(k)$ | iteration number |
| $'$ | trial phase |
| $eq$ | equilibrium |
| $res$ | residual contribution |
| $id$ | ideal contribution |

# 7 References


1. Gross, J.; Sadowski, G., Perturbed-chain SAFT: An equation of state based on a perturbation theory for chain molecules. *Industrial & engineering chemistry research* **2001,** *40*, 1244-1260.
2. Wertheim, M. S., Fluids with highly directional attractive forces. I. Statistical thermodynamics. *Journal of statistical physics* **1984,** *35*, 19-34.
3. Wertheim, M. S., Fluids with highly directional attractive forces. II. Thermodynamic perturbation theory and integral equations. *Journal of statistical physics* **1984,** *35*, 35-47.
4. Wertheim, M. S., Fluids with highly directional attractive forces. III. Multiple attraction sites. *Journal of statistical physics* **1986,** *42*, 459-476.
5. Wertheim, M. S., Fluids with highly directional attractive forces. IV. Equilibrium polymerization. *Journal of statistical physics* **1986,** *42*, 477-492.
6. De Villiers, A.; Schwarz, C.; Burger, A.; Kontogeorgis, G., Evaluation of the PC-SAFT, SAFT and CPA equations of state in predicting derivative properties of selected non-polar and hydrogen-bonding compounds. *Fluid Phase Equilibria* **2013,** *338*, 1–15.
7. Leekumjorn, S.; Krejbjerg, K., Phase behavior of reservoir fluids: Comparisons of PC-SAFT and cubic EOS simulations. *Fluid Phase Equilibria* **2013,** *359*, 17–23.
8. Peng, D.-Y.; Robinson, D. B., A new two-constant equation of state. *Industrial & Engineering Chemistry Fundamentals* **1976,** *15*, 59-64.
9. Soave, G., Equilibrium constants from a modified Redlich-Kwong equation of state. *Chemical Engineering Science* **1972,** *27*, 1197-1203.
10. Yan, W.; Varzandeh, F.; Stenby, E. H., PVT modeling of reservoir fluids using PC-SAFT EoS and Soave-BWR EoS. *Fluid Phase Equilibria* **2015,** *386*, 96-124.
11. Burgess, W. A.; Tapriyal, D.; Morreale, B. D.; Soong, Y.; Baled, H. O.; Enick, R. M.; Wu, Y.; Bamgbade, B. A.; McHugh, M. A., Volume-translated cubic EoS and PC-SAFT density models and a free volume-based viscosity model for hydrocarbons at extreme temperature and pressure conditions. *Fluid Phase Equilibria* **2013,** *359*, 38–44.
12. Schou Pedersen, K.; Hasdbjerg, C. In *PC-SAFT equation of state applied to petroleum reservoir fluids*, SPE Annual Technical Conference and Exhibition, 2007.
13. Gord, M. F.; Roozbahani, M.; Rahbari, H. R.; Hosseini, S. J. H., Modeling thermodynamic properties of natural gas mixtures using perturbed-chain statistical associating fluid theory. *Russian Journal of Applied Chemistry* **2013,** *86*, 867–878.
14. Panuganti, S. R.; Vargas, F. M.; Gonzalez, D. L.; Kurup, A. S.; Chapman, W. G., PC-SAFT characterization of crude oils and modeling of asphaltene phase behavior. *Fuel* **2012,** *93*, 658–669.
15. Zúñiga-Hinojosa, M. A.; Justo-García, D. N.; Aquino-Olivos, M. A.; Román-Ramírez, L. A.; García-Sánchez, F., Modeling of asphaltene precipitation from n-alkane diluted heavy oils and bitumens using the PC-SAFT equation of state. *Fluid Phase Equilibria* **2014,** *376*, 210–224.
16. Arya, A.; Liang, X.; Von Solms, N.; Kontogeorgis, G. M., Modeling of Asphaltene Onset Precipitation Conditions with Cubic Plus Association (CPA) and Perturbed Chain Statistical Associating Fluid Theory (PC-SAFT) Equation of States.
17. Nascimento, F. P.; Costa, G. M. N.; Melo, S. A. B. V., A comparative study of CPA and PC-SAFT equations of state to calculate the asphaltene onset pressure and phase envelope. *Fluid Phase Equilibria* **2019,** *494*, 74-92.
18. Kontogeorgis, G. M.; Folas, G. K., *Thermodynamic models for industrial applications: from classical and advanced mixing rules to association theories. Appendix A*. John Wiley & Sons: 2009.
19. Zhao, Y.; Dong, X.; Zhong, Q.; Zhang, H.; Li, H.; Shen, J.; Gong, M., Modeling Vapor Liquid Phase Equilibrium for CxHy CxHyFz Using Peng–Robinson and Perturbed-Chain SAFT. *Industrial & Engineering Chemistry Research* **2017,** *56*, 7384-7389.
20. Vidal, A.; Rodriguez, C.; Koukouvinis, P.; Gavaises, M.; McHugh, M. A., Modelling of Diesel fuel properties through its surrogates using Perturbed-Chain, Statistical Associating Fluid Theory. *International Journal of Engine Research* **2018**, 146808741880171.

21. Carneiro, A. P.; Held, C.; Rodríguez, O.; Sadowski, G.; Macedo, E. A., Solubility of Sugars and Sugar Alcohols in Ionic Liquids: Measurement and PC-SAFT Modeling. *The Journal of Physical Chemistry B* **2013,** *117*, 9980-9995.
22. Abolala, M.; Peyvandi, K.; Varaminian, F.; Hashemianzadeh, S. M., A comprehensive description of single-phase and VLE properties of cryogenic fluids using molecular-based equations of state. *Fluid Phase Equilibria* **2019,** *494*, 143-160.
23. Diamantonis, N. I.; Boulougouris, G. C.; Mansoor, E.; Tsangaris, D. M.; Economou, I. G., Evaluation of Cubic, SAFT, and PC-SAFT Equations of State for the Vapor–Liquid Equilibrium Modeling of CO2 Mixtures with Other Gases. *Industrial & Engineering Chemistry Research* **2013,** *52*, 3933-3942.
24. Rodriguez, C.; Koukouvinis, P.; Gavaises, M., Simulation of supercritical diesel jets using the PC-SAFT EoS. *The Journal of Supercritical Fluids* **2019,** *145*, 48-65.
25. Vidal, A.; Koukouvinis, P.; Gavaises, M. In *On the effect of realistic multicomponent diesel surrogates on cavitation and in-nozzle flow*, IMechE, 2018.
26. Polívka, O.; Mikyška, J., Compositional modeling in porous media using constant volume flash and flux computation without the need for phase identification. *Journal of Computational Physics* **2014**, 149-169.
27. Jindrová, T., *Computational methods in thermodynamics of multicomponent mixtures.* Master degree thesis, Czech Technical University in Prague: 2013.
28. Michelsen, M. L., The isothermal flash problem. Part I. Stability. *Fluid Phase Equilibria* **1982,** *9*, 1-19.
29. Nichita, D. V.; de-Hemptinne, J.-C.; Gomez, S., Isochoric Phase Stability Testing for Hydrocarbon Mixtures. *Petroleum Science and Technology* **2009,** *27*, 2177-2191.
30. Levy, A. V.; Gómez, S., The tunneling method applied to global optimization. *Numerical optimization* **1985,** *1981*, 213-244.
31. Mikyška, J.; Firoozabadi, A., A new thermodynamic function for phase-splitting at constant temperature, moles, and volume. *AIChE Journal* **2010,** *57*, 1897-1904.
32. Jindrová, T.; Mikyška, J., General algorithm for multiphase equilibria calculation at given volume, temperature, and moles. *Fluid Phase Equilibria* **2015,** *393*, 7-25.
33. Nichita, D. V., New unconstrained minimization methods for robust flash calculations at temperature, volume and moles specifications. *Fluid Phase Equilibria* **2018,** *466*, 31-47.
34. Paterson, D.; Michelsen, M. L.; Yan, W.; Stenby, E. H., Extension of modified RAND to multiphase flash specifications based on state functions other than (T,P). *Fluid Phase Equilibria* **2018,** *458*, 288-299.
35. Tang, X.; Gross, J., Renormalization-group corrections to the perturbed-chain statistical associating fluid theory for binary mixtures. *Industrial and Engineering Chemistry Research* **2010**, 9436-9444.
36. Bymaster, A.; Emborsky, C.; Dominik, A.; Chapman, W. G., Renormalization-group corrections to a perturbed-chain statistical associating fluid theory for pure fluids near to and far from the critical region. *Industrial and Engineering Chemistry Research* **2008**, 6264-6274.
37. García-Sánchez, F.; Schwartzentruber, J.; Ammar, M. N.; Renon, H., Modeling of multiphase liquid equilibria for multicomponent mixtures. *Fluid phase equilibria* **1996,** *121*, 207-225.
38. Schnabel, R. B.; Eskow, E., A Revised Modified Cholesky Factorization Algorithm. *SIAM Journal on Optimization* **1999,** *9*, 1135-1148.
39. Jindrová, T.; Mikyška, J., Fast and robust algorithm for calculation of two-phase equilibria at given volume, temperature, and moles. *Fluid Phase Equilibria* **2013,** *353*, 101-114.
40. von Solms, N.; Michelsen, M. L.; Kontogeorgis, G. M., Computational and Physical Performance of a Modified PC-SAFT Equation of State for Highly Asymmetric and Associating Mixtures. *Industrial & Engineering Chemistry Research* **2003**, 1098-1105.
41. Nocedal, J.; Wright, S., *Numerical Optimization*. Springer New York: 2006.
42. Fletcher, R., *Practical methods of optimization*. John Wiley & Sons: 2013.
43. Baker, L. E.; Pierce, A. C.; Luks, K. D., Gibbs Energy Analysis of Phase Equilibria. *Society of Petroleum Engineers Journal* **1982,** *22*, 731-742.

44. Mikyška, J.; Firoozabadi, A., Investigation of mixture stability at given volume, temperature, and number of moles. *Fluid Phase Equilibria* **2012,** *321*, 1-9.
45. Nichita, D. V., Fast and robust phase stability testing at isothermal-isochoric conditions. *Fluid Phase Equilibria* **2017,** *447*, 107-124.
46. Wilson, G. M. In *A modified Redlich-Kwong equation of state, application to general physical data calculations*, 65th National AIChE Meeting, Cleveland, OH, 1969; p 15.
47. Privat, R.; Gani, R.; Jaubert, J. N., Are safe results obtained when the PC-SAFT equation of state is applied to ordinary pure chemicals? *Fluid Phase Equilibria* **2010**, 76-92.
48. Press, W. H.; Flannery, B. P.; Teukolsky, S. A.; Vetterling, W. T.; Gould, H., Numerical Recipes, The Art of Scientific Computing. *American Journal of Physics* **1987,** *55*, 90-91.
49. Dahms, R. N.; Manin, J.; Pickett, L. M.; Oefelein, J. C., Understanding high-pressure gas-liquid interface phenomena in Diesel engines. *Proceedings of the Combustion Institute* **2013,** *34*, 1667-1675.
50. Mueller, C. J.; Cannella, W. J.; Bays, J. T.; Bruno, T. J.; DeFabio, K.; Dettman, H. D.; Gieleciak, R. M.; Huber, M. L.; Kweon, C.-B.; McConnell, S. S., Diesel surrogate fuels for engine testing and chemical-kinetic modeling: Compositions and properties. *Energy & Fuels* **2016,** *30*, 1445-1461.
51. Yarborough, L., Vapor-liquid equilibrium data for multicomponent mixtures containing hydrocarbon and nonhydrocarbon components. *Journal of Chemical & Engineering Data* **1972,** *17*, 129-133.
52. Kuenen, J. P., On Retrograde Condensation and the Critical Phenomena of Two Substances. *Commun. Phys. Lab U. Leiden* **1892**.
53. Liang, X., On the efficiency of PT Flash calculations with equations of state. *Computer Aided Chemical Engineering* **2018**, 859-864.
54. Chu, T.-C.; Chen, R. J. J.; Chappelear, P. S.; Kobayashi, R., Vapor-liquid equilibrium of methane-n-pentane system at low temperatures and high pressures. *Journal of Chemical & Engineering Data* **1976,** *21*, 41-44.
55. Garcia-Cordova, T.; Justo-Garcia, D. N.; Garcia-Flores, B. E.; Garcia-Sanchez, F., Vapor-Liquid Equilibrium Data for the Nitrogen - Dodecane System at Temperatures from (344 to 593) K and at Pressures up to 60 MPa. *Journal of Chemical & Engineering Data* **2011,** *56*, 1555-1564.
56. Gross, J.; Sadowski, G., Application of the perturbed-chain SAFT equation of state to associating systems. *Industrial and Engineering Chemistry Research* **2002**, 5510-5515.
57. Gross, J.; Vrabec, J., An equation-of-state contribution for polar components: Dipolar molecules. *AIChE Journal* **2006**, 1194-1204.
58. Gross, J., An equation-of-state contribution for polar components: Quadrupolar moleculesc. *AIChE Journal* **2005**, 2556-2568.
59. Shahriari, R.; Dehghani, M. R.; Behzadi, B., Thermodynamic modeling of aqueous ionic liquid solutions using PC-SAFT equation of state. *Industrial and Engineering Chemistry Research* **2012**, 10274-10282.